



Bioclimatic stress index: A tool to evaluate climate change impact on Mediterranean arid ecosystems

P. Santibáñez^a, R. Zamora^b, J. Franchi^b, D. Montaner-Fernández^a, F. Santibáñez^{a,*}

^a Facultad de Ciencias de la Naturaleza, Universidad San Sebastian, Campus Los Leones, Santiago, Chile

^b Centro de Agricultura y Medio Ambiente, Universidad de Chile, Santiago, Chile

ARTICLE INFO

Keywords:

Bioclimatic stress

Water stress

Thermal stress

Chilean ecosystems

Mediterranean ecosystems

Climate change

ABSTRACT

This study assesses the impact of mid-21st century climate change on Chile's Mediterranean sclerophyllous forests, increasingly exposed to bioclimatic stress. A novel Bioclimatic Stress Index (BSI) was developed, using 1970–2000 as a baseline and 2050 as a future scenario. Trends in bioclimatic stress and vegetation vigor were analyzed from 1986 to 2024 using the Normalized Difference Vegetation Index (NDVI), a satellite-derived measure of vegetation health and productivity. The BSI shows a significant increasing trend ($\tau = 0.3968$, $p < 0.01$), while NDVI exhibits a marked decline ($\tau = -0.433$, $p < 0.01$), indicating worsening ecosystem conditions. Key stressors include rising maximum temperatures ($+1.5^\circ\text{C}$) and increasing water deficits ($+100\text{ mm/year}$), which reduce canopy density, reproductive capacity, and overall ecosystem resilience. Unlike traditional species distribution models, the BSI quantifies climatic stress by integrating thermal and water stress into a mechanistic framework. Identifying critical stress thresholds, it provides actionable insights for conservation planning, emphasizing the urgency of adaptive strategies. The BSI's ability to quantify stress intensity rather than just predicting habitat shifts makes it a valuable tool for resilience-building interventions. Incorporating bioclimatic modeling into conservation efforts is essential to mitigate degradation, safeguard biodiversity, and enhance ecosystem resilience under future climate conditions.

1. Introduction

The geographic distribution and structure of ecosystems are predominantly shaped by bioclimatic factors, particularly temperature and water availability (Guerin et al., 2019; Luoto et al., 2005; Naudiyal et al., 2021; Sabith Rehman et al., 2024). In addition to these climate drivers, local environmental conditions such as soil properties, biotic interactions, and the adaptive capacities of species play a crucial role in determining ecosystem composition and resilience (Silva and Lambers, 2021). In Mediterranean ecosystems, species distribution is primarily constrained by thermal and water regimes, which exert selective pressures on vegetation structure and function (Casadesús et al., 2022). The thermal regime is characterized by the extreme temperature range between the warmest and coldest months, while the water regime is mainly influenced by the intensity of summer drought, which directly correlates with the annual water deficit (Grossman, 2022; Salesa et al., 2022).

Despite covering only 2 % of the global land surface, Mediterranean ecosystems harbor approximately 20 % of the world's vascular plant diversity (Arianoutsou et al., 2013). Chile's central region forms part of

this biome (Rundel et al., 2016) and has experienced rapid climatic shifts, marked by increasing temperatures and declining precipitation, leading to rising bioclimatic stress (Zhao et al., 2021). These hotter and drier summers have been shown to reduce growth rates and reproductive success in many plant species, triggering vegetation decline and ecosystem regression.

Numerous studies have analyzed the impacts of climate change on global ecosystems (Higgins et al., 2023; Li et al., 2018), with a specific focus on Latin America and the Caribbean due to the high biodiversity of the region (Uribe Botero, 2015). Mediterranean ecosystems are among the most vulnerable to these changes, as they are often located near desert boundaries, making them particularly susceptible to prolonged droughts and rising temperatures (Ji et al., 2023; Seneviratne et al., 2021). Abrupt climate variations impose ecophysiological stress on species, pushing them beyond their evolutionary adaptive capacities (Qiang et al., 2024). Given the unprecedented rate of climate change, many species lack the mechanisms required to cope, potentially leading to population declines and ecosystem disruptions (Serra-Diaz et al., 2014; Münzbergová et al., 2021). A critical concern is the loss of

* Corresponding author. Faculty of Natural Sciences, San Sebastian University, Lota 2465, Santiago, Chile.

E-mail address: fernando.santibanez@uss.cl (F. Santibáñez).

synchrony between climate patterns and species phenology, which could further accelerate biodiversity loss (Zhaoxu et al., 2022; Grossman, 2022).

Since 2010, Chile's central region has faced significant declines in precipitation, coinciding with sustained temperature increases and a severe water deficit (Boisier et al., 2016; Garreaud et al., 2019; Santibáñez and Santibáñez, 2007). These trends are consistent with global aridification processes (Gonzalez-Pérez et al., 2023). Future climate projections predict continued warming, particularly in valley regions, and further reductions in precipitation by mid-century (CR2, 2018; DMC, 2015; Rojas et al., 2019). Understanding how climate change affects ecosystems is critical for developing mitigation and adaptation strategies to prevent irreversible biodiversity loss. Recent studies have documented declines in biomass productivity across Chile's arid, semi-arid, and sub-humid regions (Van Leeuwen et al., 2013; Hernández et al., 2016), a phenomenon expected to intensify in the coming decades (Lo Parra et al., 2021; Zamora, 2020).

Among the most threatened ecosystems is the sclerophyllous forest of central Chile, which is experiencing increasing bioclimatic stress due to intensified aridity and temperature rise over recent decades (Miranda et al., 2020, 2023; Venegas-González et al., 2023). These climate shifts, coupled with anthropogenic pressures, have contributed to vegetation decline, reduced primary productivity, and an estimated 33 % loss in canopy cover (Cueto et al., 2025; Muñoz-Sáez et al., 2021). Satellite imagery confirms a progressive reduction in vegetation greenness across affected areas, mirroring patterns observed in other arid regions globally (Wang et al., 2022). The region between 30°S and 33°S, located along the southern edge of the Atacama Desert, features a subtropical arid and semi-arid climate influenced by a persistent high-pressure anticyclone, making it particularly sensitive to minor climatic fluctuations. This area is home to two dominant woodland communities: the *Acacia cavens* savannah and the sclerophyllous forest, both composed of drought-adapted, xerophytic species that undergo seasonal foliage loss.

To quantify the impact of climatic shifts on bioclimatic stress in these forests, we developed a Bioclimatic Stress Index (BSI), integrating maximum and minimum temperatures with annual water deficit. Unlike traditional habitat suitability models, such as MaxEnt (Phillips et al., 2006), which predict species distributions based on climatic correlations, the BSI explicitly quantifies the intensity of climate-induced stress on ecosystems. While MaxEnt provides valuable insights into potential habitat availability based on species occurrences and climatic conditions, it does not assess the magnitude of stress experienced by ecosystems nor isolate the specific climatic constraints limiting species survival. Unlike correlative models, which aggregate multiple environmental variables into a single predictive framework, the BSI separately evaluates key stressors—maximum summer temperature, minimum winter temperature, and annual water deficit—offering a more mechanistic approach to assessing climatic impacts (Moe et al., 2023). This methodological distinction enhances the capacity to design targeted conservation and management strategies for threatened Mediterranean ecosystems.

By integrating bioclimatic modeling with climate projections, this approach provides a scalable framework for identifying ecosystems at risk due to climate change, supporting species relocation efforts based on future climate analogs, and informing conservation strategies aimed at maintaining biodiversity under shifting climate conditions. The central objective of this study is to propose a simple yet robust methodology that leverages publicly available climate and satellite data to establish bioclimatic tolerance thresholds and assess future climate threats. The analysis of climate trends and associated biological responses serves as the foundation for identifying biodiversity loss hotspots, evaluating ecosystem vulnerability, and determining potential refugia for assisted conservation programs (Muñoz-Sáez et al., 2021).

2. Methodology

2.1. Study area

In Chile, more than 120 major plant formations have been identified, each representing unique associations of plant and animal species that establish mutualistic relationships for survival and ecological balance. These plant formations have been thoroughly mapped and described in terms of their specific compositions (Luebert and Pliscoff, 2022). For this study, we focused on two key formations within the Mediterranean climatic zone of Chile (between −33° and −35° Lat): The Mediterranean coastal sclerophyllous forest, characterized by the *Acacia cavens* and *Maytenus boaria* association, and the Mediterranean Andean sclerophyllous forest, represented by the *Acacia cavens* and *Baccharis paniculata* association. These formations were selected to evaluate bioclimatic stress, given their sensitivity to climatic variability and their ecological importance in maintaining biodiversity and ecosystem services within this region.

2.2. Climate data

2.2.1. Climate baseline and data sources

The Agroclimatic Atlas of Chile (Santibáñez et al., 2017) provides a detailed mapping of numerous bioclimatic variables relevant to the growth and adaptation of plant species. This dataset, originally covering climate conditions up to 2015, was updated to 2023 for this study. Key climatic variables, including maximum and minimum temperatures, annual precipitation, evapotranspiration, solar radiation, air humidity, and monthly temperature and precipitation, were interpolated using nonlinear multivariate models developed specifically for each variable. These models incorporated key geographical factors such as altitude, latitude, distance to the coast, and local topographic characteristics (e.g., slope, wind exposure, and aspect). The resulting interpolated data was mapped onto a 1 × 1 km grid, creating a high-resolution climate dataset suitable for further analysis.

To define the climatic baseline, we selected the period 1970–2000, aligning with WorldClim v2.1 (Fick and Hijmans, 2017). This baseline was chosen to represent historical climatic conditions that predate the significant warming trends and precipitation changes observed after 2000. Using more recent years (e.g., up to 2023) as a baseline would have introduced biases related to ongoing climate change, potentially distorting the assessment of future bioclimatic stress. Additionally, we incorporated meteorological station data provided by the Dirección Meteorológica de Chile (DMC), spanning the period 1986–2023. These in-situ temperature and precipitation records were used to validate the modeled climatic data and assess recent temporal climatic trends in the study area.

2.2.2. Global climate projections and downscaling methodology

Future climate projections were obtained from WorldClim v2.1, which provides downscaled CMIP6 climate scenarios at a spatial resolution of 1 × 1 km. We selected the Shared Socio-economic Pathway (SSP) 585 scenario for the period 2040–2060, based on an ensemble of 23 global climate models (GCMs). This high-emission scenario was used as a reference to analyze potential future climatic stress on ecosystems. This scenario was selected because it provides a reference framework that captures the maximum potential climatic impact on ecosystems, thereby allowing us to assess how habitats might respond under extremely adverse climatic conditions. To estimate future climate conditions, we calculated climatic deltas (i.e., projected changes) between the WorldClim baseline (1970–2000) and the future SSP 585 projections. These deltas were then applied to our high-resolution interpolated climate baseline, ensuring that projected future changes were spatially consistent with localized climate variations. Although WorldClim v2.1 provides a widely used global climate baseline, it does not fully capture Chile's complex climatic variability. Due to Chile's highly

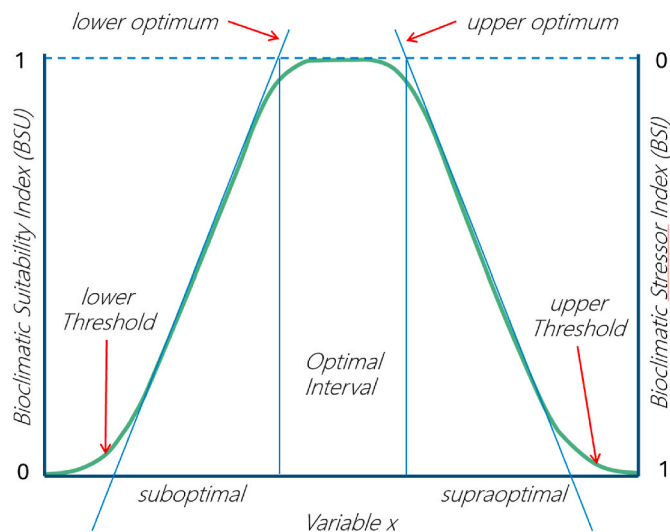


Fig. 1. Example of a bioclimatic histogram illustrating the distribution of a bioclimatic variable in the territory occupied by a species or ecosystem. The lower and upper thresholds, as well as the lower and upper optima, are the key parameters used to evaluate bioclimatic stress when the variable falls outside the optimal range. These parameters contribute to the calculation of the Bioclimatic Suitability Index (BSI) and the Bioclimatic Stress Index (BSI) within the bioclimatic stress evaluation protocol.

heterogeneous topography, there are abrupt climatic transitions between regions, resulting in localized cold and warm microclimates that are often not well represented in the WorldClim baseline. For a detailed description of the development of the high-resolution climate baseline used in this study, including the methodologies for data interpolation and validation, refer to the complementary document *High-Resolution Climate Dataset*.

2.3. Estimation of bioclimatic profile of the ecosystem

Geographic distribution of a species and plant communities are strongly determined by thermal and water regime, especially the extreme seasons (Mingxing et al., 2024; Stewart et al., 2021). Extreme temperatures are well represented by the mean maximum temperature of the warmest month and the mean minimum temperature of the coldest month. Considering the fact that precipitation is subject to different seasonality in different places, from a bioclimatic point of view it is important to consider, as a factor of plant adaptation, the integrated water deficit along the whole year. The greater the annual water deficit, the greater the aridity load that the plants must endure.

By superimposing the distribution area of a specific plant formation on this grid, the points belonging to the territory of the studied formation were selected. This selected set of data was used to characterize the bioclimatic profile of each plant formation. To establish the bioclimatic profile of each plant formation, three frequency histograms were analyzed: maximum temperature of the warmest month, minimum temperature of the coldest month and annual water deficit, the last, representing the degree of aridity, which is very sensitive to climate change in this region. The same procedure was used on the basis of present climate, and future climate, so as to calculate the displacement of the histograms in the future scenario. For each variable the optimal interval, where suitability was maximized, was defined as the range between low and high boundaries of the interval of modal frequency. All points where a climatic variable falls outside this optimal interval are considered climatically degraded, representing a suboptimal condition. This suboptimal condition is associated with increasing levels of bioclimatic stress. The degree of stress due to each variable, evaluated at each point of the spatial grid, is proportional to distance between the

boundaries of the optimum interval and the actual value of the corresponding variable. If a variable, as consequence of climate change moves within the modal interval, it will not be considered as a factor of stress. The basic assumption is that the highest presence of a plant formation occurs in the intervals where the bioclimatic suitability is more favorable, which implies null or low levels of stress. The bioclimatic suitability index (BSU) within the optimal interval is 1. Outside the optimal interval, the value of BSU_x gradually falls as the variable X moves away from the upper or lower limit of the optimal interval (Santibáñez et al., 2015). Considering that the interval with the highest frequency would be the least stressful range for the species, and that the minimum and maximum extreme values of the distribution would be associated with maximum levels of tolerated stress, a linear function is established that makes the stress grow between the extreme values of the distribution and the lower and upper borders of the interval considered non-stressful (Fig. 1).

The level of bioclimatic stress (BSI) induced by the climatic variable X outside the optimal interval is then the numerical complement value of the BSU_x:

$$BSI = 1 - BSU_x$$

To parameterize each histogram representing the bioclimatic preferences of an ecosystem, four milestones were established: lower threshold, lower bioclimatic optimum, upper bioclimatic optimum and upper threshold. Each of these milestones was associated respectively with the percentiles 2, 15, 85 and 98 % of the histogram. These calculations were performed through a routine that was programmed with R free software version 4.1.2 (R Core Team (2021)).

This procedure is applied to each of the three climatic variables used to characterize bioclimatic stress.

Integrated bioclimatic stress is calculated based on its three components

$$TBS = TX_{stress} + TN_{stress} + WD_{stress}$$

where.

TBS = total bioclimatic stress.

TX_{stress} = bioclimatic stress induced by the displacement of summer high temperatures.

TN_{stress} = bioclimatic stress induced by the displacement of winter low temperatures.

WD_{stress} = bioclimatic stress induced by the displacement of the annual water deficit (PPa-Eta).

Although the geographic dispersion of a species depends not only on the climate but also on other determinants such as biotic interactions, evolutionary changes in the environment and the competitive ability of each species (Pearson and Dawson, 2003). The three climatic drivers used in this work seem to be strongly determining factors in the distribution of the species.

2.4. Evaluation of stress levels induced by climate variations

The evaluation of bioclimatic stressors is done on a scale from 0 (no stress, the variable is within the optimal range) to 1 (maximum stress, the variable is outside the maximum interval of the territorial distribution of the species). The bioclimatic stressor index (BSI), induced by the variable x, BSI_x tend towards 0 within the optimal interval defined by the lower and the upper optimum. Between the lower optimum and the minimum threshold, the BSI_x vary from 1 to zero. In the same way, between the upper optimum and the maximum threshold. Above the maximum threshold and below the minimum threshold the bioclimatic stressor index is equal to 1

Between the lower optimum and the minimum threshold:

$$BSI_x = 1 - \frac{(V_i - V_{lower\ threshold})}{(V_{lower\ optimum} - V_{lower\ threshold})}$$

Table 1

Statistical analysis of the climatic trends in the official Met Station in Santiago (CHILE) Quinta Normal $-33^{\circ}26'42''$; $-70^{\circ}40'57''$, altitude: 534 asl (National Meteorological Service, DMC).

	Period	Annual mean	ST deviation	R	P-value
Precipitation, mm	1900–2023	326	68.1	−0.486	<0.001
Maximum temperature, °C	1911–2023	22.5	0.7	0.441	<0.001
Minimum temperature, °C	1911–2023	8.2	0.7	0.459	<0.001
Reference Evapotranspiration, mm	1946–2023	1423	129.4	0.568	<0.001
Water deficit, mm	1946–2023	−1141	217.1	−0.449	<0.001

All variables are expressed on annual basis.

Between the upper optimum and the maximum threshold:

$$BSI_x = 1 - \frac{(V_i - V_{upper\ optimum})}{(V_{upper\ threshold} - V_{upper\ optimum})}$$

This protocol was applied for calculation of the three sources of bioclimatic stressors (summer temperatures, winter temperatures and aridity) following the below algorithm.

- If $V_i < V_{lower\ threshold}$ then $BSI_x = 1$
- if $V_{lower\ threshold} < V_i < V_{lower\ optimum}$ then $BSI_x = 1 - \frac{(V_i - V_{lower\ threshold})}{(V_{lower\ optimum} - V_{lower\ threshold})}$
- if $V_{lower\ optimum} < V_i < V_{upper\ optimum}$ then $BSI_x = 0$
- if $V_{upper\ optimum} < V_i < V_{upper\ threshold}$ then $BSI_x = 1 - \frac{(V_i - V_{upper\ optimum})}{(V_{upper\ threshold} - V_{upper\ optimum})}$
- if $V_i > V_{upper\ threshold}$ then $BSI_x = 1$

This algorithm was applied to each variable at each point of the climate grid, in order to calculate the three stress indices. In this way, there was a stress induced by high summer temperatures (BSI_{summer}), by the rigor of winter cold (BSI_{winter}) and by the degree of seasonal aridity (BSI_{arid}) corresponding to the present climate and future climatic scenarios. They were integrated using an additive model in which each of them contributes to the global bioclimatic stressors which summarizes the effect of climatic drivers operating on a specific ecosystem.

The integrated bioclimatic stressors index (IBSI) was then obtained according to the following relationship:

$$IBSI = \alpha * BSI_{summer} + \beta * BSI_{winter} + \gamma * BSI_{arid}$$

$$1 = \alpha + \beta + \gamma$$

α , β and γ , are weighting coefficients for each of the 3 sources of bioclimatic stress, depending on the sensitivities of each ecosystem. In the case of the ecosystems studied, we have considered equal weights.

The final IBSI was standardized between 0 and 1 by dividing by 3 the IBSI, resulting in the standardized bioclimatic stress index (BSI), calculated at each point of the geographical grid.

$$BSI = \frac{IBSI}{3}$$

In qualitative terms, we classified the final value of the BSI into five categories: 0 to 0.2 corresponding to very low bioclimatic stress, 0.21 to 0.4 to low stress, 0.41 to 0.6 to moderate stress, 0.61 to 0.8 to high stress, and 0.81 to 1 was interpreted as very high bioclimatic stress. For more detailed refer to the complementary document *Flow Chart*.

2.5. Assessing ecosystem greenness as an indicator of bioclimatic stress

Climate change impact models can be validated by their ability to explain present conditions based on past climate trends. The underlying assumption is that observed climate variations in the region are already influencing ecosystem dynamics. To test this hypothesis, NDVI time series (greenness) were analyzed in relation to temperature and precipitation data across selected ecosystems.

Study areas were selected within sclerophyllous forest ecosystems

located in protected zones: La Campana National Park (-32.972° lat, -71.126° lon) and the Río de Los Cipreses National Reserve (-34.27° lat, -71.45° lon). These locations were chosen because land use has remained unchanged for over 60 years, as verified through land use maps provided by the Natural Resources Information Center (CIREN), which have been continuously monitored. It is of great importance that the vegetation observation sites have not been subject to human intervention, so that the observed biological changes are a real response to bioclimatic factors.

To assess bioclimatic stress over time, LANDSAT satellite images from the United States Geological Survey (USGS) (<https://earthexplorer.usgs.gov/>) were analyzed. The dataset spans 1986 to 2023, comprising 54 processed images used to calculate the Normalized Difference Vegetation Index (NDVI) in a standardized manner. These LANDSAT images already incorporate preprocessing steps, including atmospheric corrections and outlier filtering, applied according to USGS protocols. The analysis focused on a 37-year time series of monthly NDVI values, with particular attention to February, the driest month of the year. This period was chosen as it best represents NDVI variations in perennial vegetation, particularly within the sclerophyllous forest biome, where seasonal grass growth influences NDVI in other months.

Additionally, MODIS NDVI images obtained through Google Earth Engine (GEE) were analyzed for the period 2000–2023. These pre-processed MODIS products incorporate standard atmospheric corrections and outlier filtering based on NASA protocols, offering a comprehensive monthly view of vegetation changes. This dataset complements the long-term LANDSAT analysis, providing insights into seasonal and interannual trends within the sclerophyllous forest biome (Schulz et al., 2017).

2.6. Wavelet coherence analysis for evaluating bioclimatic stress-vegetation dynamics

Wavelet coherence analysis was applied to assess the dynamic relationship between the Bioclimatic Stress Index (BSI) and NDVI of the driest month of the year (Elsanabary et al., 2021). This method identifies temporal scales (e.g., short- or long-term cycles) where these associations are statistically significant, making it particularly suitable for non-stationary climatic and vegetation variables. By analyzing time-frequency dependencies, wavelet coherence provides detailed insights into the scale-dependent interactions between climate-induced stress and vegetation response.

Statistical significance thresholds were determined using Monte Carlo simulations at a 95 % confidence level. Surrogate time series were generated through phase-randomized bootstrapping, estimating expected coherence under the null hypothesis of no relationship between the two signals. In wavelet coherence analysis, black contours indicate statistically significant regions, highlighting temporal scales where the relationship between BSU (1 - BSI) and NDVI exceeds random variability. The 95 % confidence level follows standard time-frequency analysis practices, ensuring that observed coherence patterns are robust and unlikely to result from random fluctuations. This visualization offers a comprehensive representation of how bioclimatic stress influences vegetation dynamics across different temporal scales.

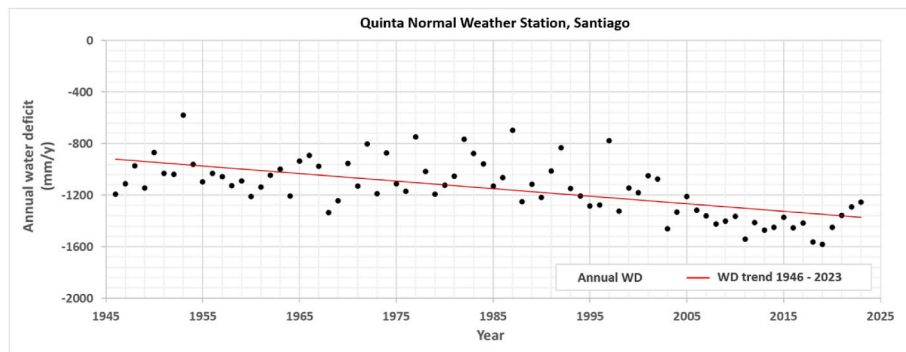


Fig. 2. Annual water deficit (annual rainfall – reference evapotranspiration) trend in Santiago area (temperate semiarid Mediterranean climate, $-33^{\circ}26'$, $-70^{\circ}41'$).

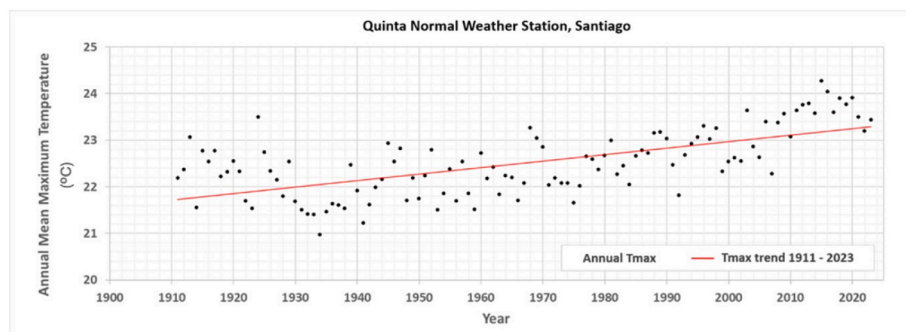


Fig. 3. Annual mean maximum temperature trend in Santiago area (temperate semiarid Mediterranean climate, $-33^{\circ}26'$, $-70^{\circ}41'$).

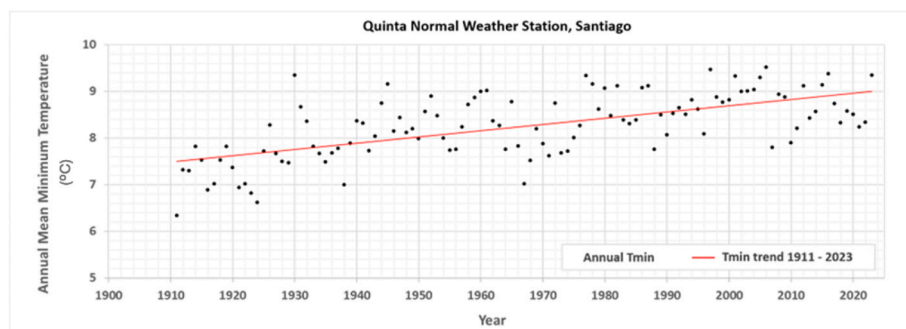


Fig. 4. Annual mean minimum temperature trend in Santiago area (temperate semiarid Mediterranean climate, $-33^{\circ}26'$, $-70^{\circ}41'$).

3. Results and discussion

3.1. Climatic trends

In recent decades, as a consequence of the southward displacement of the anticyclone of the southeast Pacific, annual precipitation (Ap) has decreased between 15 and 25 % in the central region of Chile (Table 1). Along with this trend, evapotranspiration (Eta) has risen by 10–15 % in the last 80 years. These trends have pushed the climate towards greater aridity, which is expressed in an increasingly negative water deficit (Ap-Eta, Fig. 2). This aridization is aggravated by a greater concentration of rainfall, in less frequent but more intense events. These trends are common to all polar edges of subtropical deserts in the world. Together with these trends in the water regime, the rise in temperature is causing more frequent heat waves, as well as an increase in the frequency of abnormally high temperatures for the region (Figs. 3 and 4). The statistical significance of these trends was assessed using the non-parametric Mann-Kendall test (Table 1). This method was chosen because precipitation data deviate from normality, often showing

skewness, heteroscedasticity, and temporal variability. Unlike parametric tests, the Mann-Kendall test is distribution-free and robust for detecting monotonic trends, making it well-suited for precipitation analysis.

In most of the analyzed territory, a warming of close to 1.5°C is observed, which has modified the historical climate of each ecosystem. To this it is added a displacement of the winter thermal regime, which leaves a significant fraction of the territory occupied by each ecosystem with clearly more temperate winters, a situation that is not known by these ecosystems either. Both summer heat stress and winter warming can induce ecophysiological dysfunctions that affect competitive capacity and cause a sharp regression of the species. These dysfunctions are expressed through slower annual growth, decreased canopy density, premature leaf drop, decreased chlorophyll content and, in certain cases, floral infertility. These thermal regime changes will be enhanced in the future with an increase in aridity, which should be expressed with an increase in the water deficit of around 100 mm/year and a possible lengthening of the dry season, which can lead to situations that the species are not prepared to face, reaching the mortality of

Table 2

Bioclimatic thresholds and optimal temperature and water deficit ranges for Mediterranean Thorny and Coastal Sclerophyllous Forests, derived from the spatial distribution of geographic points within each ecosystem for the baseline period (1970–2000).

	Lower Threshold	Lower Optimum	Upper Optimum	Upper Threshold
Max. Temp of the warmest month °C				
Mediterranean Thorny Forest	28.5	28.8	31.4	31.5
Mediterranean Coastal Sclerophyllous Forest	20.5	21.9	30.4	31.3
Min. Temp of the coldest month °C				
Mediterranean Thorny Forest	1.6	2.3	4	4.4
Mediterranean Coastal Sclerophyllous Forest	3.2	3.6	5.7	6.9
Water deficit (mm)				
Mediterranean Thorny Forest	−1283	−1264	−1068	−1042
Mediterranean Coastal Sclerophyllous Forest	−1133	−1105	−793	−654

individuals in sites more exposed to drought (Zhao et al., 2021).

According to global models, these climate variations will continue to accentuate in the coming decades, with summers becoming warmer, winters less cold and the climate of the central Mediterranean zone of Chile more arid, where an average rise of 1.5 °C additional to the 1.5 °C already observed in the last 80 years, and a decline in precipitation of

the order of 15–20 % towards the second half of this century (Seager et al., 2024; Zittis et al., 2023). Due to the rate and intensity of the changes that the local climate is experiencing, several ecosystems in the central region of Chile could be left in a climatic condition significantly different from the historical one, which could trigger a process of degradation, of which there is already noticeable evidence. Greater aridity, together with the higher summer temperatures, increases the levels of bioclimatic stress, which reduces the growth of trees, hinders their reproduction, and decreases the ground cover, accelerating the evaporation of water (Lozia et al., 2023). Less cold winter temperatures can also reduce the vigor and prolificacy of the flora in spring in those species that have winter dormancy, while favoring the earlier attack of pests and diseases. Several other eco-physiological processes, such as nutrient uptake from the soil, root growth, photosynthetic rates, and water balances that regulate stomatal opening, are likely to be negatively altered, leading to the weakening of the tree species that make up the ecosystem, giving way to other more rustic and aggressive species.

3.2. Estimation of bioclimatic profile of the ecosystem

The association of *Acacia cavens* and *Maytenus boaria* occupies a coastal territory that is subject to the following bioclimatic limits: average maximum temperatures of the warmest month between 20.5 and 31.3 °C, average minimum temperature of the coldest month between 3 and 7 °C and water deficit between −650 mm/year in the less arid sectors of the coast, and −1.100 mm/year the more arid sectors of the inlands (Table 2 and Fig. 5). The association of *Acacia cavens* and *Baccharis paniculata* occupies a continental territory located between the following bioclimatic limits: average maximum temperatures of the warmest month between 28 and 31.5 °C, average minimum temperature of the coldest month between 1.6 and 4.4 °C and water deficit between −1040 mm/year in the less arid sectors and −1300 mm/year in the

Mediterranean coastal thorny forest of *Acacia cavens* and *Maytenus boaria*

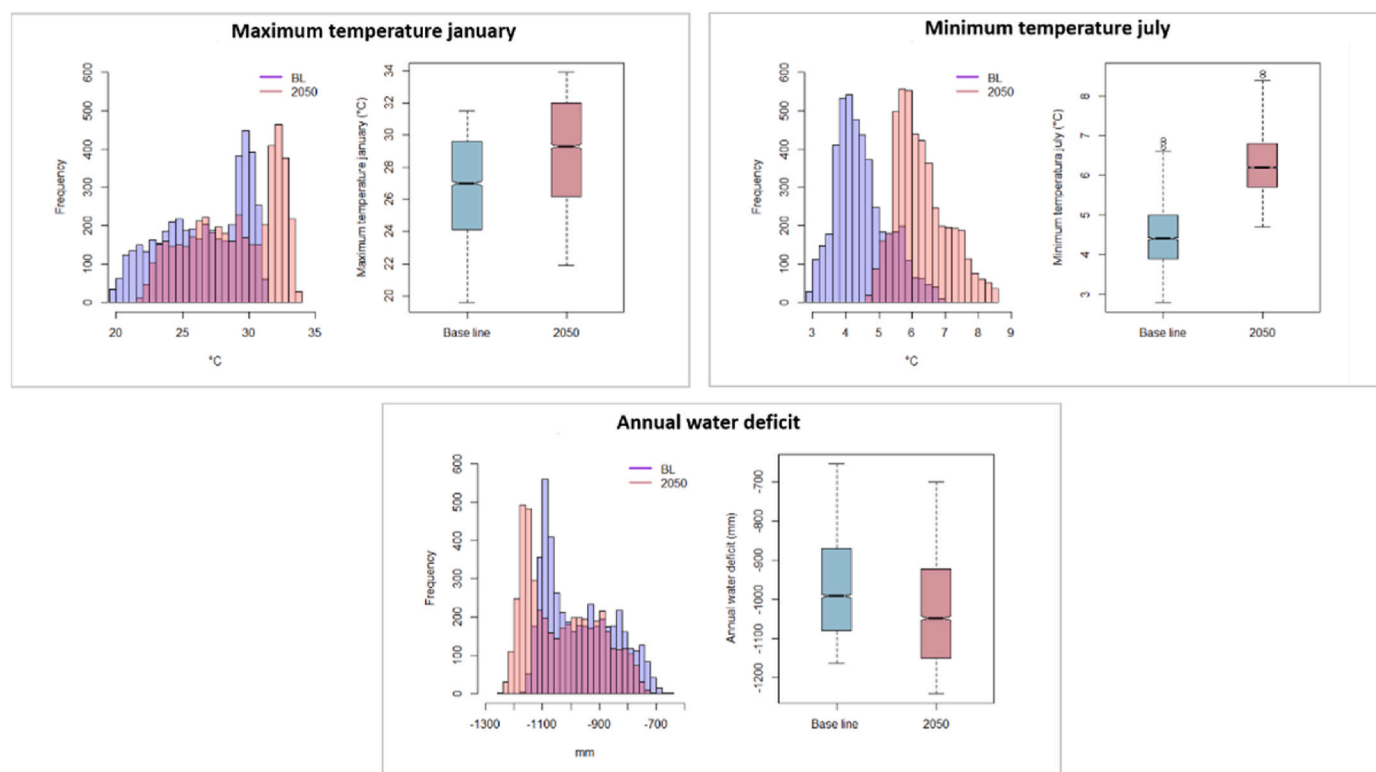


Fig. 5. Niche bioclimatic profile of the Mediterranean coastal sclerophyllous forest (*Acacia cavens* and *Maytenus boaria* association). Spatial distribution of bioclimatic variables under baseline (1970–2000) and projected (2050) climate conditions. The variables shown are the maximum temperature of January, the warmest month of the year (top left), the minimum temperature of July, the coldest month of the year (top right), and the annual water deficit (bottom).

Mediterranean Andean thorny forest of *Acacia caven* and *Baccharis paniculata*

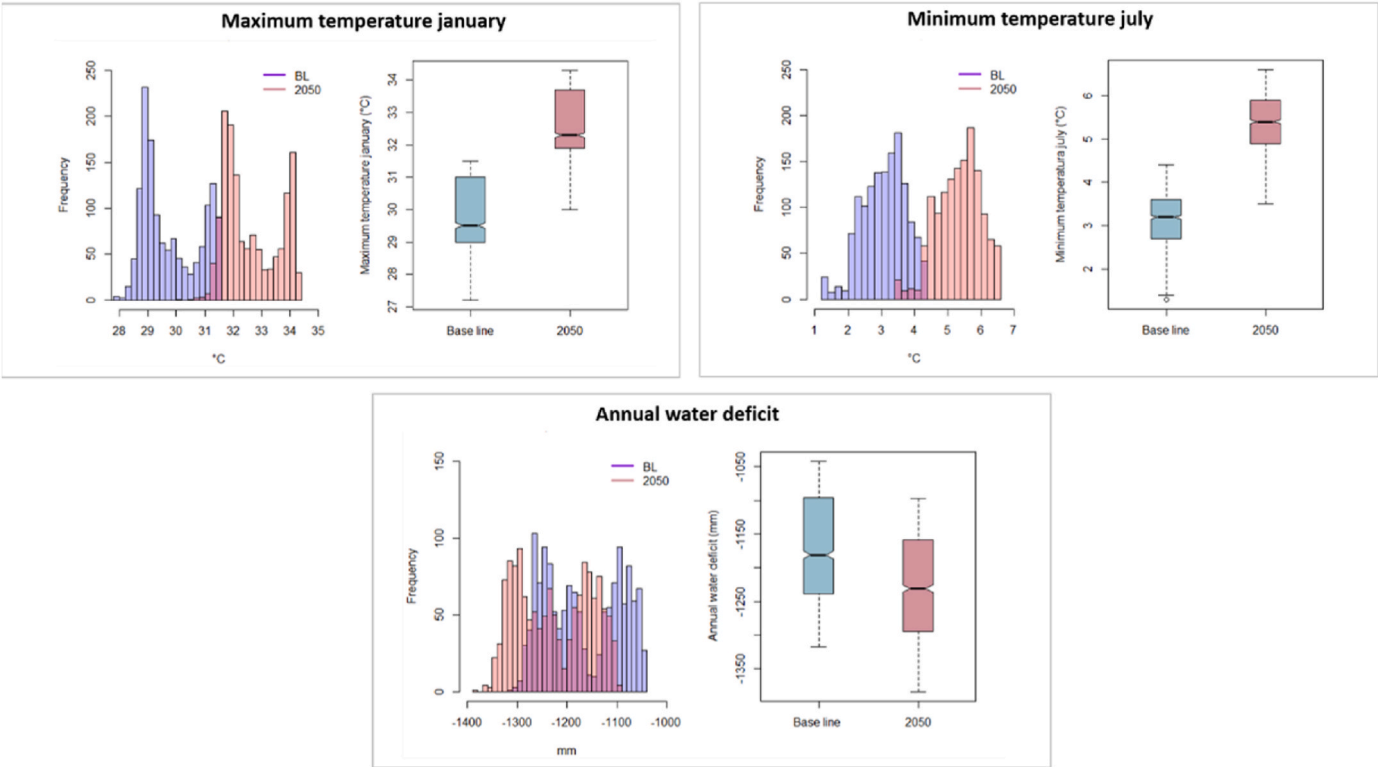


Fig. 6. Niche bioclimatic profile of the Mediterranean Andean thorny forest (*Acacia caven* and *Baccharis paniculata* association) under baseline (1970–2000) and projected (2050) climate conditions. The variables shown include maximum temperature of January (top left), minimum temperature of July (top right), and annual water deficit (bottom).

Table 3
Detection of long-term trends in NDVI anomalies and bioclimatic stress index (BSI) using the mann-kendall test.

Variable	Kendall's Tau	P-value	95 % CI (Lower)	95 % CI (Upper)
NDVI Anomalies for the Driest Month (February) During 1986–2023	−0.2804	0.038	−0.5429	−0.018
BSI (Bioclimatic Stress Index) During 1986–2023	0.3968	0.0032	0.1344	0.6593
NDVI Monthly Anomalies for the Period 2000–2024	−0.4374	0	−0.4772	−0.3976

more continental sectors (Table 2 and Fig. 6).

The maximum and minimum temperatures would experience an increase of around 1.5 °C from the reference period (1961–1990) to the 2040–2060 scenario. In the interior sectors, maximum temperatures increase 1.9 °C. The water deficit would experience, between both scenarios, an increase of 100 mm/year in coastal sectors and 140 mm/year in inland sectors. Assuming that each stress acts independently, which is the most favorable condition, the rise in maximum temperature would be responsible for an increase in thermal stress of the order of 10 % towards the 2050 scenario. The increase in minimum temperatures would be less stressful than the maximums, but more extreme episodes of cold in winter are seen in recent years, corresponding to extraordinarily cold winters caused by the incursion of polar air. The most severe

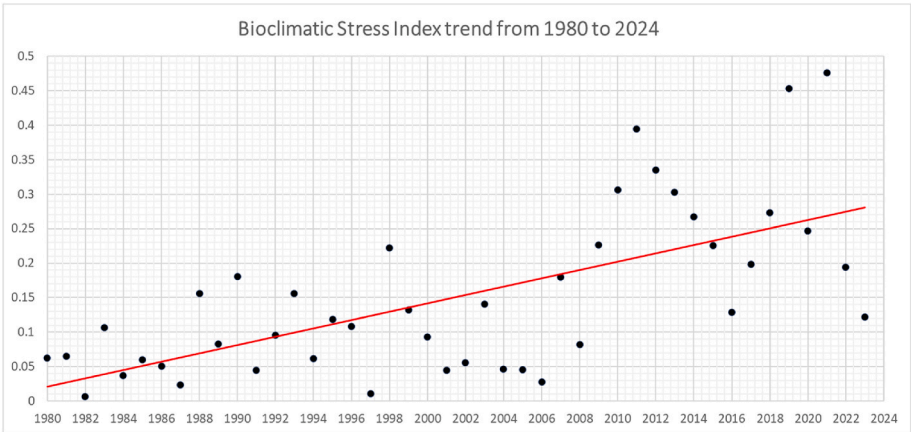


Fig. 7. Trend of the Bioclimatic stress index (BSI) over the last 40 years in the Mediterranean zone of Chile (Kendall's tau = 0.3968, p-value <0.001).

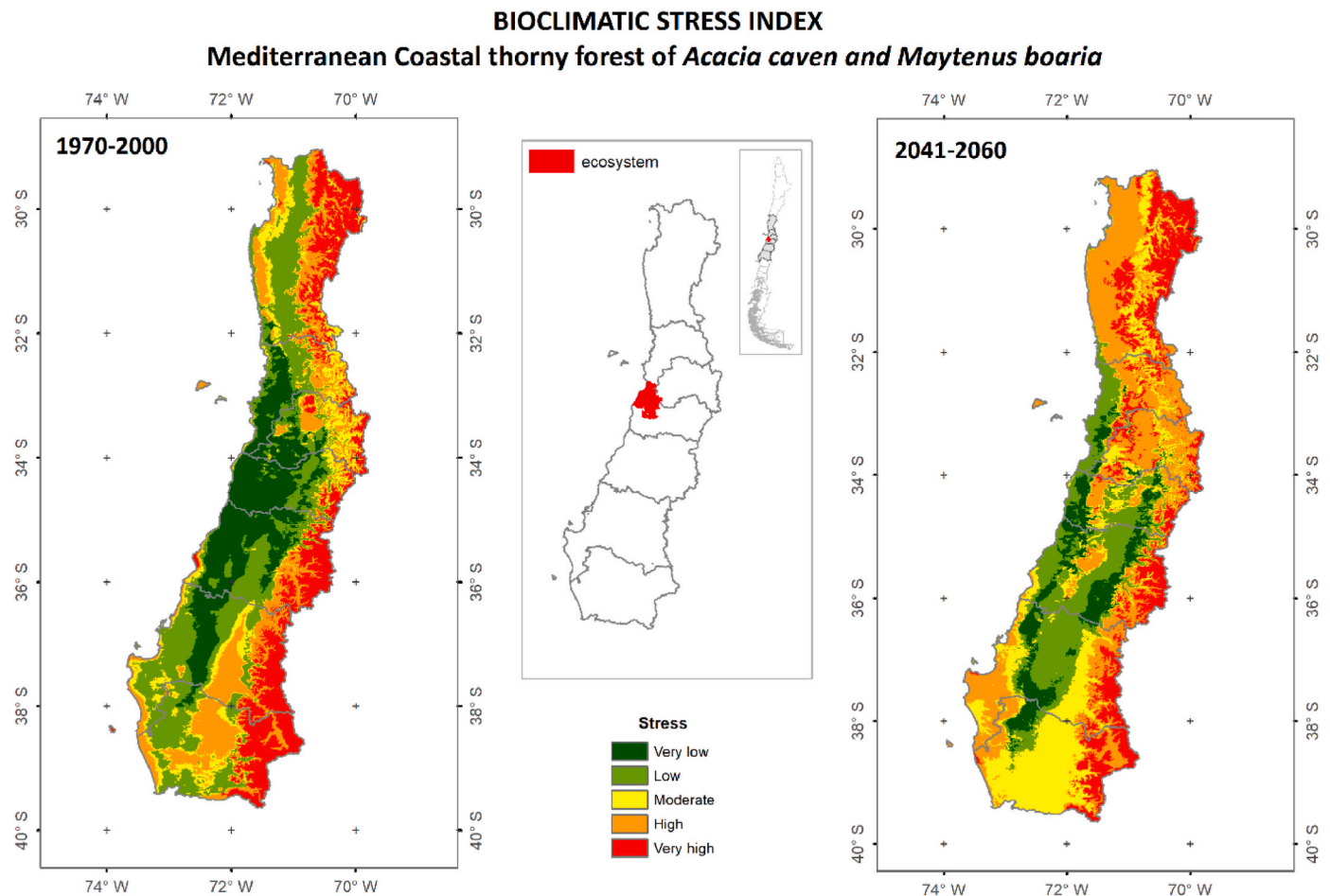


Fig. 8. Bioclimatic stress index (BSI) for the Mediterranean Coastal Sclerophyllous Forest (*Acacia cavens* and *Maytenus boaria* association). The figure illustrates the projected changes of stress index (BSI) in the central region of Chile. The left panel represents the baseline period (1970–2000), while the right panel projects the future scenario for 2041–2060.

picture of stress would be caused by the increase in water stress, which in the last 15 years has shown particularly intense episodes, associated with an extensive drought (2009–2021) that has affected this ecosystem, which has been locally called “megadrought”.

3.3. Evaluation of climate-induced stress levels

3.3.1. Current climate stress on vegetation

The bioclimatic stress induced by climate variability is a major driver of vegetation decline in Mediterranean ecosystems. To quantify the expected changes in bioclimatic suitability for this plant community, the Bioclimatic Stress Index (BSI) was developed by integrating three key stressors into an additive model. The Mann-Kendall trend analysis (Table 3) reveals a significant increase in BSI ($\tau = 0.3968$, $p = 0.0032$), confirming a progressive intensification of climate-induced stress over time.

Initially, BSI showed a slight decreasing trend from 1980 to 2008. However, since 2009, there has been a sharp increase in stress levels, likely driven by heatwaves and prolonged droughts, which exacerbate both thermal and water stress. This significant rise suggests that the cumulative impact of high temperatures and water deficits could severely impair plant growth and reproduction, increasing ecosystem vulnerability (Fig. 7).

3.3.2. Projected trend of climate suitability for sclerophyllous forest in the Mediterranean climate region of Chile, in the next decades

By 2050, substantial climatic shifts are expected within this species'

habitat, requiring adaptation to unprecedented conditions. Maximum temperatures during the warmest month will rise to 34 °C, pushing a significant portion of its range beyond the current upper threshold of 32 °C. Similarly, minimum winter temperatures will increase from the current 3–7 °C range to 5–8.5 °C.

Increasing aridification will lead to a 100 mm increase in annual water deficit, surpassing the current maximum threshold of –1200 mm/year for this ecosystem. Higher temperatures and intensified drought conditions will likely compound the negative effects of thermal stress and dehydration, resulting in reduced vegetation vigor and reproductive capacity, ultimately leading to a shift in species composition.

Our analysis suggests that the bioclimatic conditions of the current ecological associations will undergo a strong contraction, particularly in inland regions, where rising temperatures and aridification will be most severe. Coastal populations will retreat to a narrower strip along the coastline, while some refugia may persist in the Andean foothills, where temperatures will be lower and conditions less arid. Notably, a new bioclimatic niche is projected to emerge further south of the current range, offering a potential relocation area for these species (Fig. 8).

Inland populations will experience a generalized decline, with no newly emerging areas suitable for assisted migration. The most favorable bioclimatic conditions will be reduced to a thin corridor along the coastal zone, signaling a significant loss of suitable habitat for this ecosystem. The increased bioclimatic stress on the sclerophyllous forest in central Chile is already evident, as seen in the browning, canopy thinning, and lack of regeneration affecting these plant communities, particularly in drier continental areas (Fig. 9).

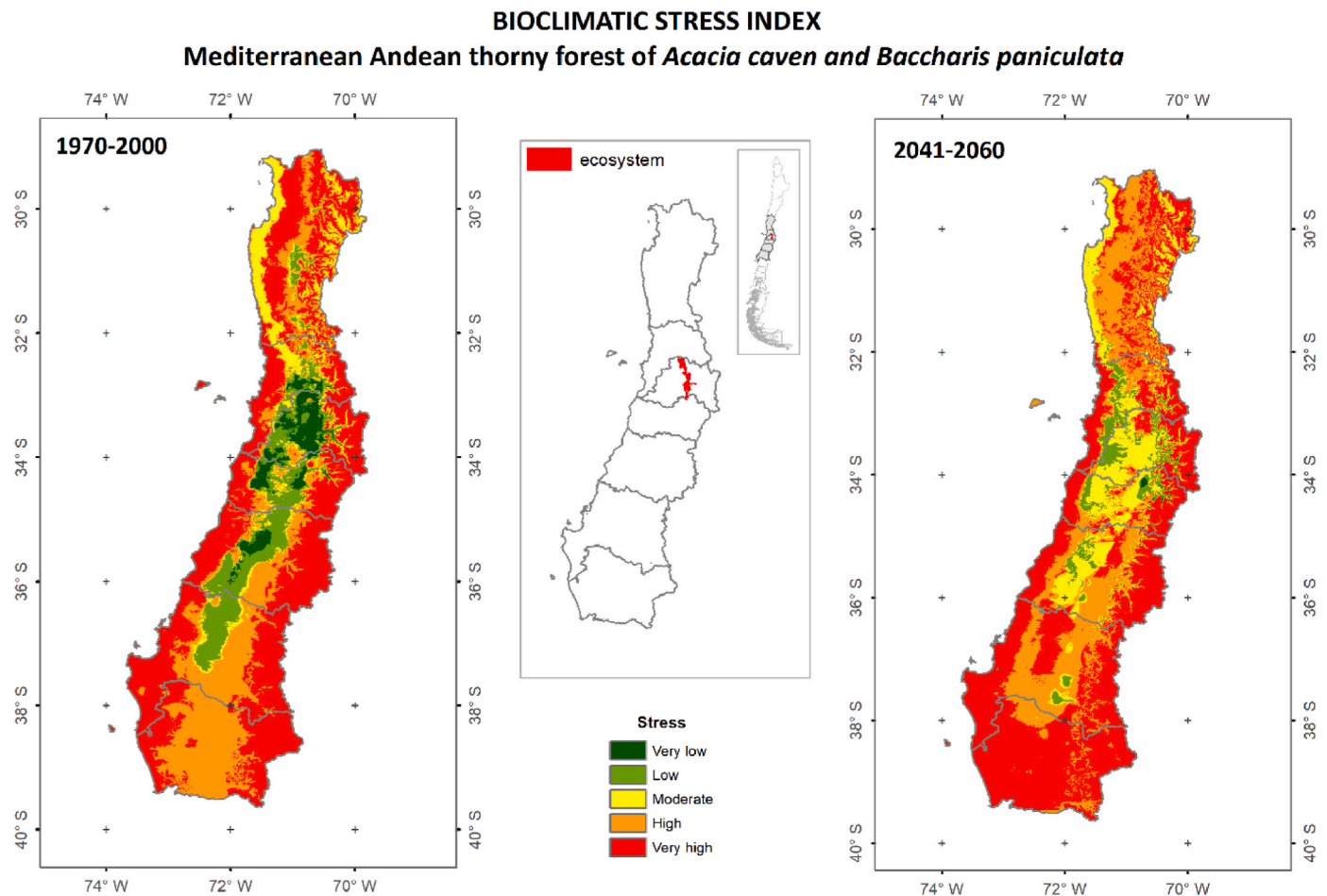


Fig. 9. Bioclimatic stress index (BSI) for the Mediterranean andean sclerophyllous forest (*Acacia cavens* and *Baccharis paniculata* association). The figure illustrates the projected changes of the stress index (BSI) in the central region of Chile. The left panel represents the baseline period (1970–2000), while the right panel projects the future scenario for 2041–2060.

This territorial analysis, integrating climate scenarios and bioclimatic modeling, can serve as a valuable tool for assisted conservation planning. Identifying future refugia and maintaining the current bioclimatic profile of key species or species associations will be crucial for ensuring ecosystem resilience in the face of climate change.

3.4. Assessing ecosystem greenness as an indicator of bioclimatic stress

The biological response of the vegetation is reflected in a widespread loss of greenness that can be captured by MODIS Terra satellite images, as shown by the Normalized Difference Vegetation Index (NDVI) monthly anomalies in Fig. 10. The application of the non-parametric Mann-Kendall test showed a τ value of -0.437 , indicating a negative correlation in the NDVI anomalies, suggesting a decreasing trend in the vegetation of the analyzed area over time, with a p-value significantly less than 0.01 (Table 3). This strong statistical evidence demonstrates a marked decrease in the vigor or extent of the sclerophyllous forest canopy in the study area during the observed period. This vegetation response is quite consistent with the projections made through the bioclimatic stress index, which considers the combined effect that drought and high temperatures will have in the future on sub-desert areas of the planet.

The Mann-Kendall trend analysis applied to NDVI anomalies for the driest month of the year (February) (Table 3) reveals a statistically significant negative trend (Kendall's tau = -0.2804 , $p = 0.038$), further supporting the overall decline in vegetation vigor over time.

This analysis specifically isolates tree canopy conditions by removing

the influence of seasonal herbaceous cover, which is entirely dry during this period, providing a more focused assessment of long-term forest degradation (Fig. 11).

3.5. Wavelet coherence analysis for evaluating bioclimatic stress-vegetation dynamics

Wavelet coherence analysis was applied to identify common frequency patterns between the Bioclimatic Stress Index (BSI) and NDVI of the driest month. This method provides a statistical measure of the correlation between two time series across different temporal scales, making it particularly suitable for analyzing non-stationary climatic and vegetation variables. BSI reflects climate-induced stress patterns, while NDVI represents the biological response of the ecosystem.

Since both signals exhibit frequency variations over time, wavelet coherence analysis was used to determine temporal scales at which climate stressors exert the strongest influence on vegetation dynamics. Unlike traditional statistical approaches that assume stationarity, this method captures both short-term fluctuations and long-term ecological trends, making it a valuable tool for climate impact assessments. Fig. 12 illustrates the high coherence between the climatic signal and the biological response, providing strong evidence that the BSI effectively captures ecophysiological changes in the sclerophyllous forest. The results indicate that.

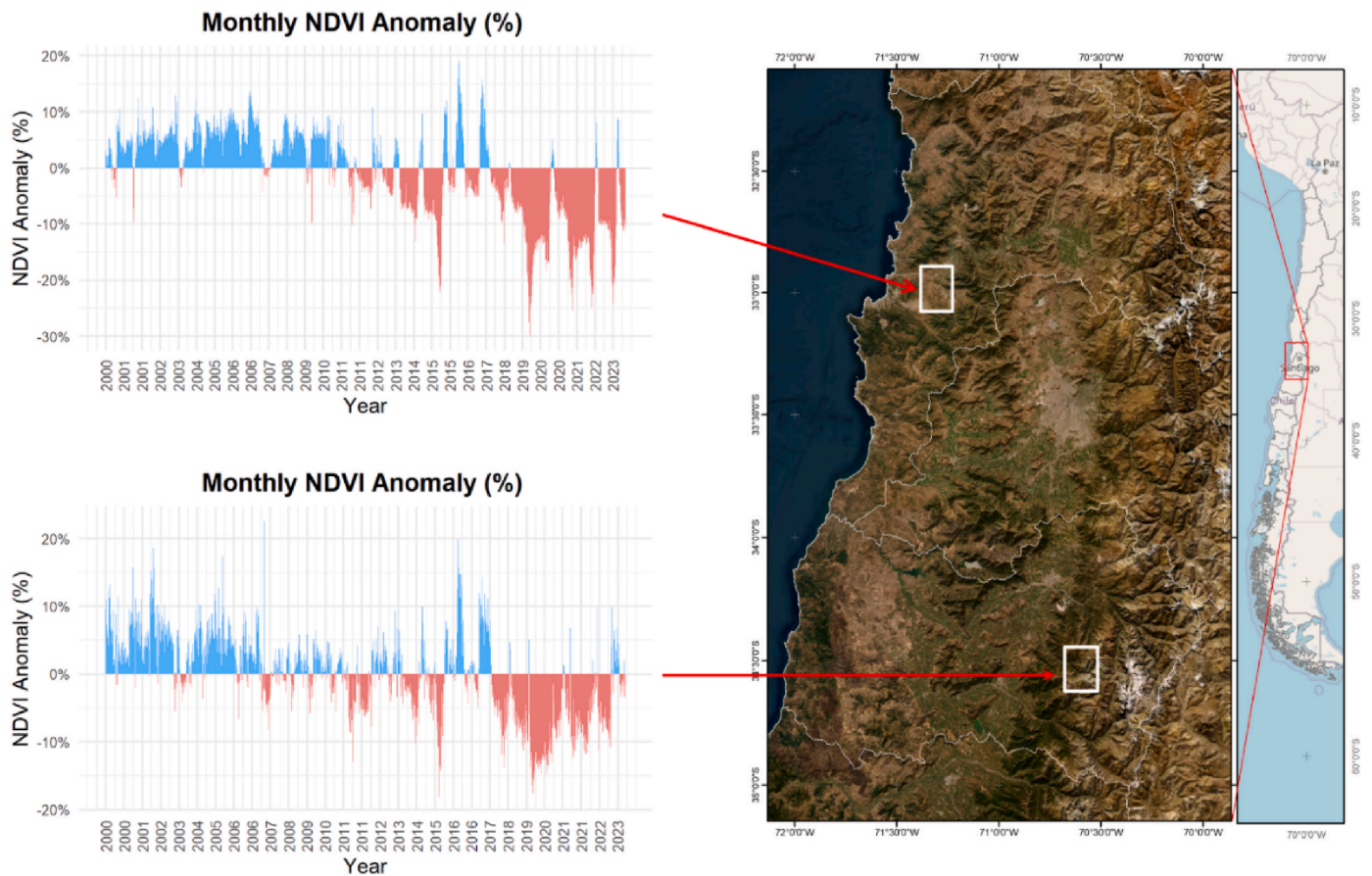


Fig. 10. NDVI anomalies (%) in the territory of the sclerophyllous forest ecosystem in La Campana National Park (-32.972° lat, -71.126° lon) and Río de Los Cipreses National Reserve (-34.27° lat, -71.45° lon), including all months of the year between 2000 and 2023.

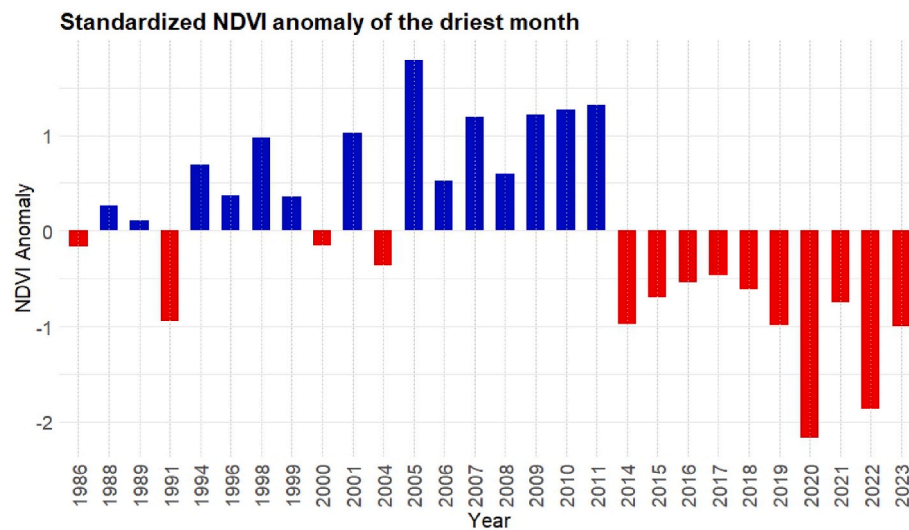


Fig. 11. Standardized NDVI anomalies for the driest month of the year (February) between 1986 and 2024, in an area of the sclerophyllous forest ecosystem in Chile, La Campana National Park (-32.972° lat, -71.126° lon).

- At long timescales (>6 years), strong coherence suggests that cumulative effects of warming and drought drive structural changes in vegetation productivity.
- At shorter timescales (2–5 years), coherence is more variable and weaker, likely influenced by interannual climatic oscillations such as El Niño or seasonal droughts. This suggests that vegetation responses to climatic stressors are not immediate but develop over extended

periods, depending on species resilience and local environmental conditions.

Climatic variations often occur over short and abrupt periods, whereas biological responses tend to lag behind and persist longer. This pattern is clearly visible in the lower portion of Fig. 12, where short-term fluctuations show lower coherence than long-term trends.

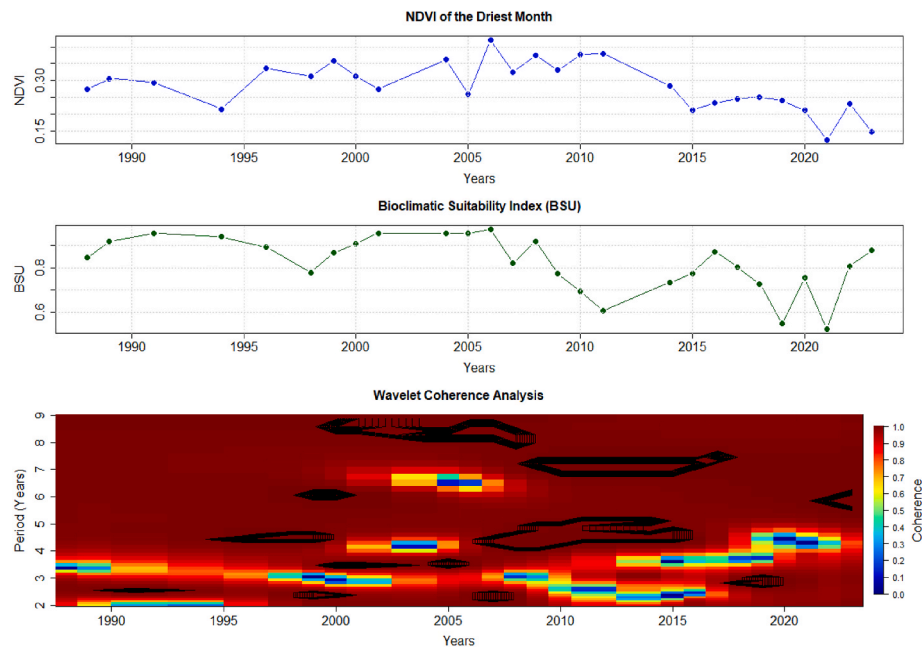


Fig. 12. NDVI of the driest month (february), Bioclimatic Suitability Index ($BSU = 1 - BSI$), and Wavelet Coherence between NDVI values and the Bioclimatic Suitability Index across time and temporal scales. The top graphs show the evolution of NDVI (blue) and BSU (green) from 1986 to 2023. The bottom graph represents the wavelet coherence analysis, where colors indicate the intensity of the relationship between both variables at different temporal scales (y-axis: period). The color gradient ranges from blue (low coherence) to red (high coherence), highlighting the strength of the association. Significant coherence regions are outlined in black, indicating statistically significant relationships at the 95 % confidence level. (For interpretation of the references to color in this figure legend, the reader is referred to the Web version of this article.)

This approach represents a key methodological advancement in linking climatic and ecological dynamics, providing a scalable and adaptable framework for assessing climate-driven ecosystem changes. The integration of wavelet coherence analysis in bioclimatic research enhances the ability to identify critical thresholds, anticipate ecosystem shifts, and guide evidence-based conservation and adaptation policies. Previous studies have demonstrated similar ecophysiological-climatic coupling (Ghaderpour et al., 2023; Zhou et al., 2022; Cheng et al., 2022; Paschalis et al., 2015).

Key Findings.

1. A simple and robust methodology, based on distribution area and historical climate mapping, to generate a profile of minimum bioclimatic requirements for species and ecosystems.
2. An integrated calculation system for bioclimatic stress is proposed, that can modify the climate in the habitat of species or ecosystems as consequence of climate change.
3. The same system could be helpful in establishing areas with emerging climates to host assisted protection programs for species threatened by climate change.
4. Reproducible methodologies that can be adapted to the parameters of different ecosystems, based on public and easily accessible information. High temperatures, as well as low temperatures and water deficit within the annual cycle, are primary bioclimatic “drivers” for the adaptation of any species. Each species has different demands and tolerances that has to be determined by overlaying its territorial distribution and the key climatic variables for the adaptation of the species. The proposed methodology is based on this, which synthesizes the habitability of a climate for a species or a complete ecosystem in an integrated index (BSI). The work proposes a methodology, based on geospatial analysis, to estimate the tolerance profile based on the characterization of the climate in the territory occupied by each biological entity (Santibáñez, 2014).

4. Conclusions

The recent climatic changes in central Chile’s semi-arid Mediterranean region show a clear trend of rising temperatures and increasing aridification, driven by declining annual rainfall and higher evapotranspiration rates. As in other arid regions worldwide, these shifts are creating stressful conditions for the sclerophyllous forest, which is already exhibiting visible signs of ecological regression.

This study highlights the high sensitivity of vegetation in arid and semi-arid Mediterranean climates to climate change. This justifies the urgent need for adaptive conservation strategies to mitigate the effects of climate change on these ecosystems. By integrating NDVI anomalies and bioclimatic profiles, we have demonstrated the impact of increasing temperatures and prolonged drought on vegetation health and species distribution. A key finding is the utility of bioclimatic profiling to assess the potential risks posed by future climate scenarios at both species and ecosystem levels. Despite potential distortions from human activities, this approach provides a practical framework for defining bioclimatic tolerance limits and identifying priority conservation areas under changing climatic conditions.

To enhance conservation planning, we advocate for an adaptive management approach that incorporates predictive methodologies, such as remote sensing and climate downscaling, to assess climate-induced bioclimatic stress. Once an ecosystem’s bioclimatic tolerance thresholds are established, this methodology can help identify future climate analogs, guiding strategic placement of assisted protection programs and species relocation efforts.

Additionally, the combination of rising temperatures and reduced precipitation is driving a decline in primary productivity, increasing vegetation mortality and altering carbon sequestration dynamics. These processes not only weaken forest resilience but also contribute to higher CO₂ emissions due to organic matter degradation. Future research should focus on quantifying biomass loss and organic matter oxidation rates, providing critical insights to refine conservation strategies and better mitigate climate impacts.

CRediT authorship contribution statement

P. Santibáñez: Writing – original draft, Methodology, Investigation, Formal analysis, Conceptualization. **R. Zamora:** Writing – original draft, Validation, Investigation, Data curation. **J. Franchi:** Visualization, Validation, Data curation. **D. Montaner-Fernández:** Writing – review & editing, Writing – original draft, Investigation. **F. Santibáñez:** Writing – review & editing, Writing – original draft, Methodology, Investigation, Funding acquisition, Conceptualization.

Funding

This work was supported by National Agency of Research and Development, Ministry of Science (CHILE) which funded the project FONDEF IDEA ID20I10135.

Declaration of competing interest

The authors declare the following financial interests/personal relationships which may be considered as potential competing interests: Fernando Santibáñez reports financial support was provided by Fund for the Promotion of Scientific and Technological Development. If there are other authors, they declare that they have no known competing financial interests or personal relationships that could have appeared to influence the work reported in this paper.

Acknowledgements

We acknowledge the National Agency of Research and Development, Ministry of Science of republic of Chile, which funded the project FONDEF IDEA ID20I10135.

This work was supported by Vicerrectoría de Investigación y Doc- torados de la Universidad San Sebastián – Fondo USS-FIN-25-APCS-13.

Data availability

Data will be made available on request.

References

- Arianoutsou, M., Delipetrou, P., Vila, M., Dimitrakopoulos, P.G., Celesti-Grapow, L., Wardell-Johnson, G., et al., 2013. Comparative patterns of plant invasions in the Mediterranean biome. *PLoS One* 8 (11), e79174. <https://doi.org/10.1371/journal.pone.0079174>.
- Boisier, J.P., Rondanelli, R., Garreaud, R.D., Muñoz, F., 2016. Anthropogenic and natural contributions to the Southeast Pacific precipitation decline and recent megadrought in central Chile. *Geophys. Res. Lett.* 43 (1), 413–421. <https://doi.org/10.1002/2015GL067265>.
- Casadesús, A., Bouchikh, R., Munné-Bosch, S., 2022. Contrasting seasonal abiotic stress and herbivory incidence in *Cistus albidus* L. plants growing in their natural habitat on a Mediterranean mountain. *J. Arid Environ.* 206, 104842. <https://doi.org/10.1016/j.jaridenv.2022.104842>.
- Cheng, X., Xu, Z., Yu, S., Peng, J., 2022. A wavelet coherence approach to detecting ecosystem services trade-off response to land use change. *J. Environ. Manag.* 316, 115160. <https://doi.org/10.1016/j.jenvman.2022.115160>.
- Cueto, D.A., Alaniz, A.J., Hidalgo-Corrotea, C., Vergara, P.M., Carvajal, M.A., Barrios-Saravia, A., 2025. Chilean Mediterranean forest on the verge of collapse? Evidence from a comprehensive risk analysis. *Sci. Total Environ.* 964, 178557. <https://doi.org/10.1016/j.scitotenv.2025.178557>.
- DMC, 2015. Análisis de los resultados convenio alta dirección pública: Director, Dirección Meteorológica de Chile, objetivo n.° 3 (p. 31). Santiago, Chile: Dirección Meteorológica de Chile. Recuperado de: <https://docplayer.es/70866380-Resumen-analisis-de-los-resultados-convenio-alta-direccion-publica-director-direccion-meteorologica-de-chile-objetivo-n-3.html>.
- Elsanabary, M.H., Khafagy, H.E., Abdellah, S.E., 2021. Rainfall variation over Sinai Peninsula and its teleconnection to El Niño sea surface temperature. *J. Arid Environ.* 193, 104581. <https://doi.org/10.1016/j.jaridenv.2021.104581>.
- Fick, S.E., Hijmans, R.J., 2017. WorldClim 2: new 1-km spatial resolution climate surfaces for global land areas. *Int. J. Climatol.* 37 (12), 4302–4315. <https://doi.org/10.1002/joc.5086>.
- Garreaud, R.D., Boisier, J.P., Rondanelli, R., Montecinos, A., Sepúlveda, H.H., Veloso-Aguila, D., 2019. The Central Chile Mega Drought (2010–2018): a climate dynamics perspective. *Int. J. Climatol.* 40 (1), 421–439. <https://doi.org/10.1002/joc.6219>.
- Ghaderpour, E., Mazzanti, P., Scarascia Mugnozza, G., Bozzano, F., 2023. Coherency and phase delay analyses between land cover and climate across Italy via the least-squares wavelet software. *Int. J. Appl. Earth Obs. Geoinf.* 118, 103241. <https://doi.org/10.1016/j.jag.2023.103241>.
- Gonzalez-Pérez, R., Alvarez-Esteban, A., Velázquez, A., Penas, S., 2023. Bioclimatic drought and its trends in California State (U.S.). *Ecol. Indic.* 153, 110426. <https://doi.org/10.1016/j.ecolind.2023.110426>.
- Guerin, G.R., Andersen, A.N., Rossetto, M., van Leeuwen, S., Byrne, M., Sparrow, B., Lowe, A.J., 2019. Consistent sorting but contrasting transition zones in plant communities along bioclimatic gradients. *Acta Oecol.* 95, 74–85. <https://doi.org/10.1016/j.actao.2019.01.006>.
- Grossman, J.J., 2022. Phenological physiology: seasonal patterns of plant stress tolerance in a changing climate. *New Phytol.* 237 (4), 1508–1524. <https://doi.org/10.1111/nph.18617>.
- Hernández, Á., Arellano, E.C., Morales-Moraga, D., Miranda, M., 2016. Understanding the effect of three decades of land use change on soil quality and biomass productivity in a Mediterranean landscape in Chile. *Catena* 140, 195–204. <https://doi.org/10.1016/j.catena.2016.01.029>.
- Higgins, S.I., Conradi, T., Muhoko, E., 2023. Shifts in vegetation activity of terrestrial ecosystems attributable to climate trends. *Nat. Geosci.* 16 (2), 147–153. <https://doi.org/10.1038/s41561-022-01119-3>.
- Ji, Y., Fu, J., Lu, Y., Liu, B., 2023. Three-dimensional-based global drought projection under global warming tendency. *Atmos. Res.* 291, 106812. <https://doi.org/10.1016/j.atmosres.2023.106812>.
- Li, D., Wu, S., Liu, L., Zhang, Y., Li, S., 2018. Vulnerability of the global terrestrial ecosystems to climate change. *Glob. Change Biol.* 24 (9), 4095–4106. <https://doi.org/10.1111/gcb.14327>.
- Lo Parra, J., Garrido Velarde, J., Barrena González, J., Pulido Fernández, M., 2021. Chapter 5. Ecohydrological behavior of semiarid ecosystems of Chile in present and future climate scenarios. In: Castanho, R.A., Gallardo, J.M. (Eds.), *Management and Conservation of Mediterranean Environments*. IGI Global, pp. 60–74. <https://doi.org/10.4018/978-1-7998-7391-4.ch005>.
- Lozia, L.M., Crisafulli, V., Varone, L., 2023. Climatic variations along an aridity gradient drive significant trait intraspecific variability in Mediterranean plant species. *J. Arid Environ.* 217, 105042. <https://doi.org/10.1016/j.jaridenv.2023.105042>.
- Luebert, F., Pliscoff, P., 2022. The vegetation of Chile and the EcoVeg approach in the context of the International Vegetation Classification project. *Vegetation Classification and Survey* 3, 15–28. <https://doi.org/10.3897/VCS.67893>.
- Luoto, M., Pöyry, J., Heikkinen, R.K., Saarinen, K., 2005. Uncertainty of bioclimate envelope models based on the geographical distribution of species. *Global Ecol. Biogeogr.* 14 (6), 575–584. <https://doi.org/10.1111/j.1466-822X.2005.00186.x>.
- Miranda, A., Lara, A., Altamirano, A., Di Bella, C., González, M.E., Camarero, J.J., 2020. Forest browning trends in response to drought in a highly threatened Mediterranean landscape of South America. *Ecol. Indic.* 115, 106401. <https://doi.org/10.1016/j.ecolind.2020.106401>.
- Miranda, A., Syphard, A.D., Berdugo, M., Carrasco, J., Gómez-González, S., Ovalle, J.F., et al., 2023. Widespread synchronous decline of Mediterranean-type forest driven by accelerated aridity. *Nat. Plants* 9 (11), 1810–1817. <https://doi.org/10.1038/s41477-023-01541-7>.
- Mingxing, L., Wu, P., Ma, Z., Liu, J., 2024. Climate change reshapes bioclimatic environments in China's dry-wet transition zones. *J. Hydrol.* 634, 131122. <https://doi.org/10.1016/j.jhydrol.2024.131122>.
- Moe, J.S., Brix, K., Landis, W.G., Stauber, J., Carriger, J.F., Hader, J.D., Kunimitsu, T., Mentzel, S., Noyes, N.P., Oldenkamp, R., Rohr, J.R., Van den Brink, P.J., Verheyen, R., Benestad, R.E., 2023. Integrating climate model projections into environmental risk assessment: a probabilistic modeling approach. *Integrated Environ. Assess. Manag.* <https://doi.org/10.1002/ieam.4879>.
- Muñoz-Sáez, A., Choe, H., Boynton, R.M., Elsen, P.R., Thorne, J.H., 2021. Climate exposure shows high risk and few climate refugia for Chilean native vegetation. *Sci. Total Environ.* 785, 147399. <https://doi.org/10.1016/j.scitotenv.2021.147399>.
- Münzbergová, Z., Vandvik, V., Hadincová, V., 2021. Evolutionary rescue as a mechanism allowing a clonal grass to adapt to novel climates. *Front. Plant Sci.* 12, 659479. <https://doi.org/10.3389/fpls.2021.659479>.
- Naudiyal, N., Wang, J., Ning, W., Gaire, N.P., Peili, S., Yanqiang, W., et al., 2021. Potential distribution of *Abies*, *Picea*, and *Juniperus* species in the sub-alpine forest of Minjiang headwater region under current and future climate scenarios and its implications on ecosystem services supply. *Ecol. Indic.* 121, 107131. <https://doi.org/10.1016/j.ecolind.2020.107131>.
- Paschalis, A., Faticchi, S., Katul, G.G., Ivanov, V.Y., 2015. Cross-scale impact of climate temporal variability on ecosystem water and carbon fluxes. *J. Geophys. Res.: Biogeosciences* 120, 1716–1740. <https://doi.org/10.1002/2015JG003002>.
- Pearson, R.G., Dawson, T.P., 2003. Predicting the impacts of climate change on the distribution of species: are bioclimate envelope models useful? *Global Ecol. Biogeogr.* 12 (5), 361–371. <https://doi.org/10.1046/j.1466-822X.2003.00042.x>.
- Phillips, S.J., Anderson, R.P., Schapire, R.E., 2006. Maximum entropy modeling of species geographic distributions. *Ecol. Model.* 190 (3–4), 231–259. <https://doi.org/10.1016/j.ecolmodel.2005.03.026>.
- Qiang, Jin, Muzafaruddin, Chachar, Aamir, Ali, Zaid, Chachar, Pingxian, Zhang, Adeel, Riaz, Nazir, Ahmed, Sadaruddin, Chachar, 2024. Epigenetic regulation for heat stress adaptation in plants: new horizons for crop improvement under climate change. *Agronomy* 14 (9). <https://doi.org/10.3390/agronomy14092105>, 2105–2105.
- R Core Team, 2021. R: A Language and Environment for Statistical Computing. R Foundation for Statistical Computing, Vienna, Austria. URL: <https://www.R-project.org/>.

- Rojas, M., Lambert, F., Ramirez-Villegas, J., Challinor, A., 2019. Emergence of robust precipitation changes across crop production areas in the 21st century. *Proc. Natl. Acad. Sci. U. S. A* 116 (14), 6673–6678. <https://doi.org/10.1073/pnas.1811463116>.
- Rundel, P.W., Arroyo, M.T., Cowling, R.M., Keeley, J.E., Lamont, B.B., Vargas, P., 2016. Mediterranean biomes: evolution of their vegetation, floras, and climate. *Annu. Rev. Ecol. Evol. Systemat.* 47, 383–407. <https://doi.org/10.1146/annurev-ecolsys-121415-032330>.
- Sabith Rehman, Z., Iqbal, Z., Qureshi, R., Khan, A.M., Qaseem, M.F., Siddiqui, M.H., 2024. Bioclimatic and remote sensing factors are better key indicators than local topography and soil: vegetation composition variability in forests of Pakistan's Spin Ghar Mountain range. *Ecol. Indic.* 153, 112111. <https://doi.org/10.1016/j.ecolind.2024.112111>.
- Salesa, D., Baeza, M.J., Pérez-Ferrándiz, E., Santana, V.M., 2022. Longer summer seasons after fire induce permanent drought legacy effects on Mediterranean plant communities dominated by obligate seeders. *Sci. Total Environ.* 806, 153655. <https://doi.org/10.1016/j.scitotenv.2022.153655>.
- Santibáñez, F., Santibáñez, P., Caroca, C., Gonzalez, P., Perri, P., Gajardo, N., 2017. Atlas agroclimático de Chile Estado actual y tendencias del clima. Universidad de Chile. Facultad de Ciencias Agronómicas, FIA, Santiago, Chile.
- Santibáñez, F., Mendoza, J., Muñoz, C., Caroca, C., Santibáñez, P., Prat, L., 2015. Systems to establish bioclimatic analogies to predict the area of adaptability of plant species to new environments: the case of *Moringa oleifera* Lam. in Chile. *Chil. J. Agric. Res.* 75 (4), 425–433. <https://doi.org/10.4067/S0718-58392015000500007>.
- Santibáñez, F., Santibáñez, P., 2007. Cambio climático y degradación de tierras en Latinoamérica y Chile. *Revista Ambiente & Desarrollo* 23 (3), 54–63.
- Seager, R., Wu, Y., Cherchi, A., Simpson, I.R., Osborn, T.J., Kushnir, Y., Nakamura, J., 2024. Recent and near-term future changes in impacts-relevant seasonal hydroclimate in the world's Mediterranean climate regions. *Int. J. Climatol.* 1–29. <https://doi.org/10.1002/joc.8551>.
- Seneviratne, S., et al., 2021. Weather and climate extreme events in a changing climate. In: Masson-Delmotte, V., et al. (Eds.), *Climate Change 2021: The Physical Science Basis*. Contribution of Working Group I to the Sixth Assessment Report of the Intergovernmental Panel on Climate Change. Cambridge University Press, Cambridge, UK. <https://doi.org/10.1017/9781009157896.013>.
- Serra-Diaz, J.M., Franklin, J., Ninyerola, M., Davis, F.W., Syphard, A.D., Regan, H.M., Ikegami, M., 2014. Bioclimatic velocity: the pace of species exposure to climate change. *Divers. Distrib.* 20 (2), 169–180. <https://doi.org/10.1111/ddi.12131>.
- Silva, L.C.R., Lambers, H., 2021. Soil-plant-atmosphere interactions: structure, function, and predictive scaling for climate change mitigation. *Plant Soil* 461 (1–2), 5–27. <https://doi.org/10.1007/s11104-020-04427-1>.
- Schulz, C., Koch, R., Cierjacks, A., Kleinschmit, B., 2017. Land change and loss of landscape diversity at the Caatinga phytogeographical domain: analysis of pattern-process relationships with MODIS land cover products (2001–2012). *J. Arid Environ.* 136, 54–74. <https://doi.org/10.1016/j.jaridenv.2016.10.004>.
- Stewart, S.B., Eliot, J., Fedrigo, M., Kasel, S., Roxburgh, S.H., Bennett, L.T., Chick, M.P., Fairman, T.A., Leonard, S., Kohout, M., Cripps, J.K., Durkin, L., Nitschke, C.R., 2021. Climate extreme variables generated using monthly time-series data improve predicted distributions of plant species. *Ecography* 44 (4), 626–639. <https://doi.org/10.1111/ecog.05253>.
- Uribe Botero, E., 2015. El cambio climático y sus efectos en la biodiversidad en América Latina. CEPAL, Santiago, Chile. Recuperado de. <https://www.cepal.org/es/publicaciones/39855-cambio-climatico-sus-efectos-la-biodiversidad-america-latina>.
- Van Leeuwen, W.J.D., Hartfield, K., Miranda, M., Meza, F.J., 2013. Trends and ENSO/AAO driven variability in NDVI derived productivity and phenology alongside the Andes Mountains. *Remote Sens.* 5 (3), 1177–1203. <https://doi.org/10.3390/rs5031177>.
- Venegas-González, A., Muñoz, A.A., Carpintero-Gibson, S., González-Reyes, A., Schneider, I., Gipolou-Zuñiga, T., et al., 2023. Sclerophyllous forest tree growth under the influence of a historic megadrought in the Mediterranean Ecoregion of Chile. *Ecosystems* 26 (2), 344–361. <https://doi.org/10.1007/s10021-022-00760-x>.
- Wang, L., Jiao, W., Rulli, M.C., MacBean, N., Manzoni, S., Vico, G., D'Odorico, P., 2022. Dryland productivity under a changing climate. *Nat. Clim. Change* 12, 981–994. <https://doi.org/10.1038/s41558-022-01499-y>.
- Zamora, R.C., 2020. Processos de desertificação associados a pastagens no Chile para o clima presente e cenários climáticos futuros (Tese de doutorado). Instituto Nacional de Pesquisas Espaciais - INPE, São José dos Campos, Brasil. Recuperado de. http://bdtd.ibict.br/vufind/Record/INPE_c0c81ed70a9b1a2276e0201d43d68170.
- Zhao, X., Liu, Z., Fang, X., Zheng, H., Zhang, L., 2021. Changes in water availability during the dry season in the Yellow River Basin, China: implications for climate change adaptation. *Front. Environ. Sci.* 9, 762137. <https://doi.org/10.3389/fevs.2021.762137>.
- Zhaoyu, G., Zhou, Y., He, Y., 2022. Molecular epigenetic mechanisms for the memory of temperature stresses in plants. *J. Genetics Genomics* 49 (11), 991–1001. <https://doi.org/10.1016/j.jgg.2022.07.004>.
- Zhou, Z., Liu, S., Ding, Y., Fu, Q., Wang, Y., Cai, H., Shi, H., 2022. Assessing the responses of vegetation to meteorological drought and its influencing factors with partial wavelet coherence analysis. *J. Environ. Manag.* 311, 114879. <https://doi.org/10.1016/j.jenvman.2022.114879>.
- Zittis, G., Urdiales-Flores, D., Cherchi, A., Hadjinicolaou, P., 2023. Projected changes in the distribution of global Mediterranean climate-type regions. EGU General Assembly 2023, EGU23–6043. <https://doi.org/10.5194/egusphere-egu23-6043>.